

5. Barker, R. W., Taxonomic notes. *Soc. Econ. Paleontol. Mineral. Spec. Publ.*, 1960, **9**, 238.
6. Loeblich, A. R. and Tappan, H., *Foraminiferal Genera and their Classification*, Nostrand Reinhold, New York, 1988, pp. 1–2.
7. Clemens, S., Prell, W., Murray, D., Shimmield, G. and Weedon, G. Forcing mechanisms of the Indian Ocean monsoon. *Nature*, 1991, **353**, 720–725.
8. Juyal, N., Chamyal, L. S., Bhandari, S., Bhushan, R. and Singhvi, A. K., Continental record of the southwest monsoon during the last 130 ka: evidence from the southern margin of the Thar Desert, India. *Quat. Sci. Rev.*, 2006, **25**, 2632–2650.
9. Leuschner, D. C. and Sirocko, F., Orbital insolation forcing of the Indian monsoon: a motor for global climate changes? *Palaeogeogr., Palaeoclimatol., Palaeoecol.*, 2003, **197**, 83–95.
10. Naidu, P. D. and Malmgren, B. A., A high resolution record of the late Quaternary upwelling along the Oman margin, Arabian Sea based on planktonic foraminifera. *Palaeoceanography*, 1996, **11**, 129–140.
11. Cushman, J. A., A Recent *Guembelitra*(?) from the Pacific. *Contrib. Cushman Found. Foram. Res.*, 1934, **10**, 105.
12. Lutze, G. F., Benthische Foraminiferen in Oberflächen-Sedimenten der Perisischen Golfes, Teil 3: Arten, *Meteor. Forschungsergebnisse C.*, 1974, **17**, 1–66.
13. Loeblich, A. R. and Tappan, H., Some new and revised genera and families of hyaline calcareous Foraminiferida (Protozoa). *Trans. Am. Microsc. Soc.*, 1986, **105**, 239–265.

ACKNOWLEDGEMENTS. This work is part of a project sponsored by the JV partnership which includes BG India, ONGC and RIL, all of whom are thanked for permission to publish this paper. We acknowledge the help extended by Goutam Ghosh, BG Exploration and Production India Ltd, during this study. The work is also a part of the IGCP Project 476 to P.K.S. The suggestions of the anonymous reviewer have helped improve the manuscript.

Received 27 March 2008; revised accepted 7 October 2008

First observations of free oscillations of the earth from Indian superconducting gravimeter in Himalaya

B. R. Arora^{1,*}, Kamal², Amit Kumar², Gautam Rawat¹, Naresh Kumar¹ and V. M. Choubey¹

¹Wadia Institute of Himalayan Geology, Dehradun 248 001, India

²Department of Earth Sciences, Indian Institute of Technology Roorkee, Roorkee 247 667, India

The first Indian superconducting gravimeter (SG) was installed in March 2007 at the Multi-Parametric Geophysical Observatory of the Wadia Institute of Himalayan Geology, in the Himalaya near the Main Central Thrust at Ghuttu, Uttarakhand, India. Almost immediately after installation, the free oscillations excited after the Solomon Islands earthquake ($M = 8.1$) were

well recorded on the SG. The frequency and amplitude of several of these oscillations have been estimated in the present study and compared with the earlier global observations. The results are in tandem with similar studies carried out using a global dataset from the seismometers and SG. The present study validates the quality of the recorded data to search minute (submicrogal) coseismic/precursory gravity signals to large earthquakes and sets the background for future low-frequency seismological research in the country. Some new applications of SG data are also discussed.

Keywords: First observations, free oscillations, Indian superconducting gravimeter.

THE first Indian superconducting gravimeter (SG) was installed at the Multi-Parametric Geophysical Observatory (MPGO) established recently by the Wadia Institute of Himalayan Geology (WIHG), at Ghuttu (30.53°N, 78.74°E), Garhwal Himalayas, Uttarakhand. Set up as a part of the Mission mode project on seismology, the MPGO is designed to study the earthquake precursors in an integrated manner¹. The MPGO is equipped with Overhauser magnetometer, tri-axial fluxgate magnetometer, magnetotelluric, SG, ULF-band induction coil magnetometer, radon data-logger, water-level recorders and is backed by the dense network of broad-band seismometers (BBS) and Global Positioning System (GPS). High-precision equipment have the requisite sensitivities to record characteristic stress-induced perturbations² in magnetization, resistivity and density in the focal zone of the impending earthquake, whereas opening of minor cracks, influx of fluids and material strengthening during the earthquake preparatory cycle can be searched through the distinct space-time patterns in micro-seismicity, seismic wave-velocity alterations, crustal deformation, anomalous electromagnetic and inert gas emission as well as by rapid changes in hydro-dynamical parameters. The first installation of the SG at Ghuttu has been carried out with the ultimate objective of monitoring minute (submicrogal-level) variations in the gravity field of the earth due to small tectonic deformations and/or mass redistribution arising due to strain accumulation in association with the on-going collision between India and Asia, and to study co-seismic/precursory gravity signals, if any, to a large earthquake³.

In principle, the design of the SG-sensing element is similar to an inverted spring-mass system. A small, superconducting spherical mass levitates on the magnetic field of a loop current in a superconducting coil. Any change in gravity, however small, causes a vertical shift in the position of the sphere that can be recorded. The detailed working procedure of the SG can be found in Goodkind⁴. Figure 1 shows the internal structure of the gravity-sensing unit (inset) as well as various components of the SG supplied by M/s GWR, USA. The complete gravity-sensing unit (GSU) that includes superconducting magnets, a niobium sphere, temperature-control circuitry and

*For correspondence. (e-mail: arorabr@wihg.res.in)

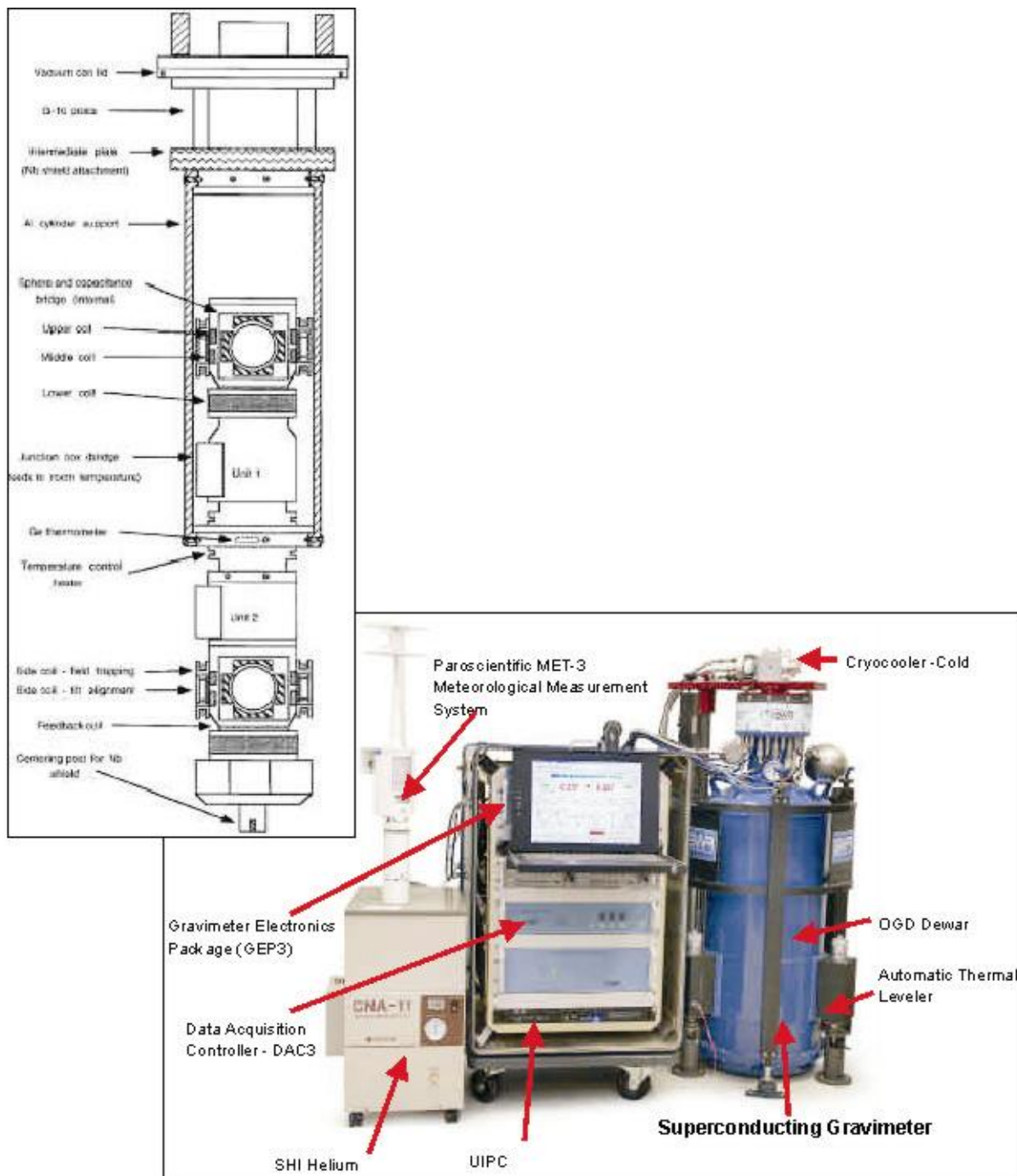


Figure 1. Various components of the superconducting gravimeter (SG) installed at (MPGO), Ghuttu. (Inset) Description of the superconducting sensor which lies inside the OGD Dewar.

magnetic shielding are housed in the liquid helium tank (Dewar) and an external refrigeration system, including cold head and helium compressor keeps the GSU close to 4.2 K to maintain the superconducting state. The supporting equipment includes gravimeter electronic package (GEP), data acquisition controller (DAC), a pair of cryogenic tilt meters, an automatic tilt-compensating system, a current supply/heater pulser, a helium-level sensor, a liquid helium management system, GPS which corrects the

timing system every second and a meteorological measurement system (MET). The atmospheric pressure sensor is part of the MET equipment that is required to remove the effect of pressure on gravity data. It has been also shown that measured gravity variations⁵ are sensitive to changes in groundwater level. The MPGO is also equipped with a water-level recorder and hence the concurrent data can be used to estimate and remove the effect of hydrological parameters on the measured gravity variations on a regu-

lar basis. Since its development in the late sixties⁶, the SG has been used to monitor very long period signals such as earth tides, polar motion, surface deformation and mass shifts^{3,7,8}. No other gravity-measuring instrument approaches the accuracy of the SG, so that it is almost impossible to calibrate it at the claimed accuracy of nGal ($1 \text{ nGal} = 10^{-3} \mu\text{Gal} = 10^{-11} \text{ m/s}^2$) level. However, at about $10 \mu\text{Gal}$ level, it is compared with the theoretical solid earth tides for calibration. Reliable algorithms⁹ are available to calculate the theoretical solid earth tide at a given location and altitude. Further comparison with the recently inducted absolute gravimeter on the Indian scene⁴ would permit calibration at $2 \mu\text{Gal}$ level and help in establishing the drift character of the SG.

The sudden release of energy in a very large earthquake can set the entire earth into vibration at numerous discrete mode frequencies that are determined by the elastic properties and structure of the earth's interior¹⁰. In a bounded elastic body approximated to first order a sphere (e.g. the earth), the superposition of travelling surface waves along the surface results in a stationary interference pattern, which is equivalent to a system of standing waves. This set of standing waves, whose wavelengths on and in the earth are an integral multiple of the circumference of the earth, is termed free oscillations of the earth (FOE). The free oscillations involving radial, spheroidal and toroidal modes produce complex three-dimensional deformation in the earth. The records of long-period seismograms excited by distant, large earthquakes are extensively used to characterize the frequency, amplitude, phase and decay factor for the range of FOE¹¹⁻¹³. The departures of the observed frequencies of normal modes from their theoretical values are used to provide a measure of asphericity, lateral heterogeneity and deviation from spherical symmetry of the earth, whereas decay factor of damping FOE provides a measure of anelasticity in the deep interior. The results of such exercises are used to define the Preliminary Reference Earth Model¹⁴. Given the working equivalence of the SG with a seismometer, the high sensitivity and sampling rate of the SG are exploited to characterize fundamental modes of the FOE¹¹. Since SG responds to only vertical motion, only spheroidal modes of the FOE are quantified by gravity variations. The SG data were first tested in the normal mode band¹¹ and the quality (decay) factors of several fundamental spheroidal modes of the earth, excited after the Indonesia earthquake of 18 April 1990 were provided. The Indian SG is the most sensitive instrument in the country suitable for carrying out such analysis. Immediately after the installation of the Indian SG in late March 2007, a large earthquake of magnitude 8.1 (M_s) occurred on 1 April 2007 (20:39:56 UTC) near Solomon Islands (8.6°S , 157.2°E with an epicentral distance of 84.26°). In this communication, we provide frequencies of several spheroidal oscillations excited by this great earthquake in the SG data recorded at Ghuttu. The periods of many FOE,

including the gravest mode ${}_0\text{S}_2$ and breathing mode ${}_0\text{S}_0$ show reasonable agreement with earlier studies¹¹⁻¹³ and validate the quality of the data recorded for envisaged objectives with the continuous long-period data being registered.

The MPGO is located in the Garhwal Lesser Himalaya sequence immediately south of the Main Central Thrust (MCT), where hard granitic gneisses of Chail Formation are the dominant rock types¹⁵. It is embedded in the narrow zone of concentrated seismicity centred (Figure 2) around the MCT¹⁶. This segment of the Garhwal Himalaya falls in the central seismic gap¹⁷ where two large earthquakes have occurred in the last one and half decade, viz. 1991 Uttarkashi (M_b 6.6) and 1999 Chamoli (M_b 6.8). The recent GPS measurements also indicate that the sector is stressed critically to produce one or more great earthquakes¹⁸.

The Indian SG is among the few SGs around the globe that record the gravity values at high sampling rates. The response of the MODE filter of the SG is sampled and digitized at 1 sample/s. The sampling time is picked up through a GPS clock installed with the SG. The scale factor of the Indian SG in the present study is assumed to be the same as of that of the Canadian SG GWR-12 used earlier¹¹. The dominant component of the signal is attributed to the solid earth tides, which has a range of about $145 \mu\text{Gal}$. The background noise recorded in the data is about $0.4 \mu\text{Gal}$.

Figure 3a shows a 48 h record of the SG incorporating the period of the Solomon Islands earthquake. The time variations expectedly were dominated by the long-period semi-diurnal lunar tides. However, against these periodic oscillations, the seismic signals from this earthquake

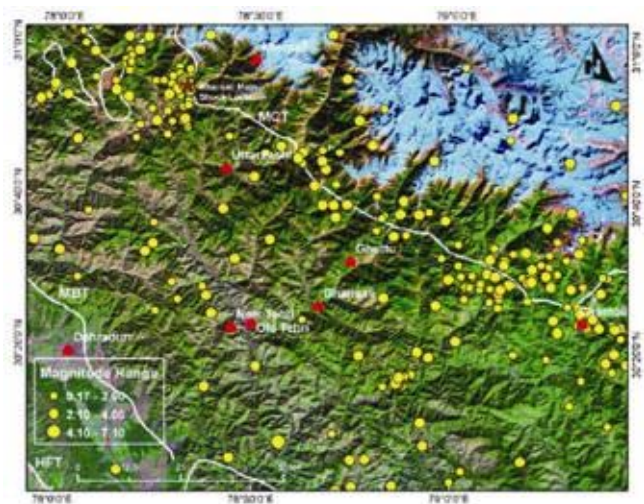


Figure 2. Location map of the First Indian MPGO at Ghuttu in relation to mega thrusts of the Himalaya, namely Main Central Thrust (MCT), Main Boundary Thrust (MBT) and Himalayan Frontal Thrust (HFT). Yellow circles mark the epicentres of earthquakes recorded between July 2007 and July 2008.

were recorded on the Indian SG with a range of about 1500 μGal . Many seismic phases from this earthquake were clearly visible on the SG record (Figure 3). The FOE are made up from infinite number of decaying sinusoids. This decaying nature introduces errors in amplitude estimation through conventional Fourier analysis. We have avoided this by estimating local amplitude in successive overlapping windows. The local amplitude estimate of each sinusoid was obtained in each segment and the attenuation, in terms of the quality factor Q , was estimated using the change in the amplitude of a particular frequency in successive windows. The minimum length of the segment for complex frequency estimation was 1.1 Q cycles¹⁹. Following this practice, the segment length was chosen as 24 h. The Rayleigh phases from the earthquake exhibited saturation on the records and this portion of the data was excluded from the analysis. We selected our first 24 h of time window well after the subsidence of this saturation zone. The first time window analysed started 3 h after the first P -arrival of the Solomon Islands

earthquake at the Indian SG site and successive overlapping windows were selected with a shift of 1.5 h. A multi-radix FFT routine was used to compute the Fourier transform, which does not require any zero padding in the data.

The SG has an equivalence with the vertical component of a seismometer in that it responds only to the vertical changes of gravity. Therefore, only the spheroidal modes can be observed on SG records. Figure 4 shows the amplitude spectrum of three successive overlapping 24-h time windows starting after about 3 h of the first P -arrival of the Solomon Islands earthquake at the Indian SG site. The spheroidal modes have been identified by matching their periods with the earlier global observations obtained by stacking global records¹² and single stations^{11,13}. The periods of spheroidal modes observed in the present study have been compared with the earlier results in Table 1. All the periods observed on the Indian SG were well within 1% of the earlier results (Figure 5).

It is also evident from Figure 4 that the amplitude of the FOE decreases with time. The amplitudes of the

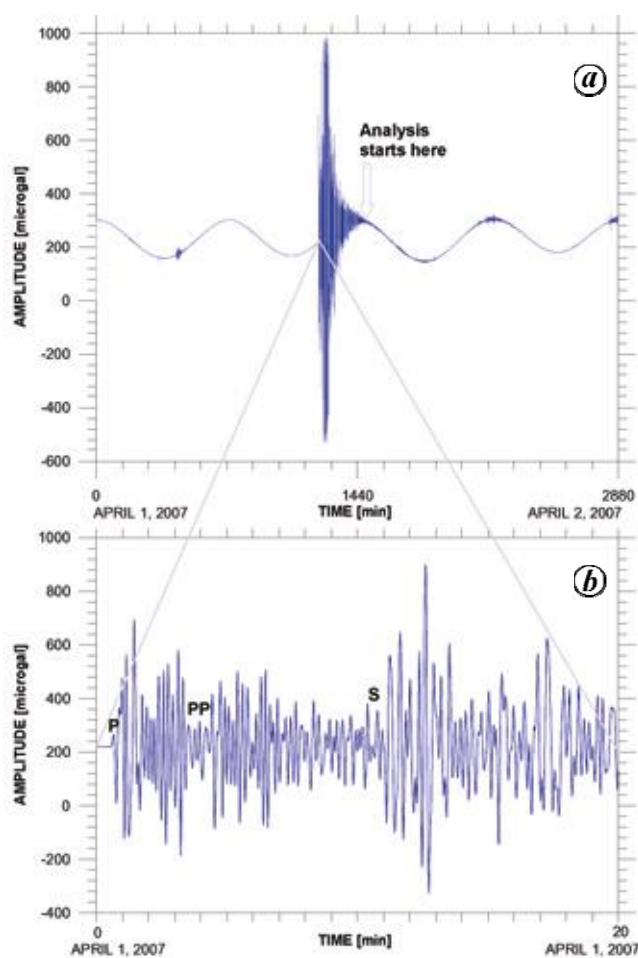


Figure 3. *a*, A 48 h record of the SG during the Solomon Islands earthquake of 1 April 2007 ($M_S = 8.1$, epicentral distance = 84.26°). *b*, A 20 min plot of the SG record showing the arrival times of some early earthquake phases for the Solomon Islands earthquake.

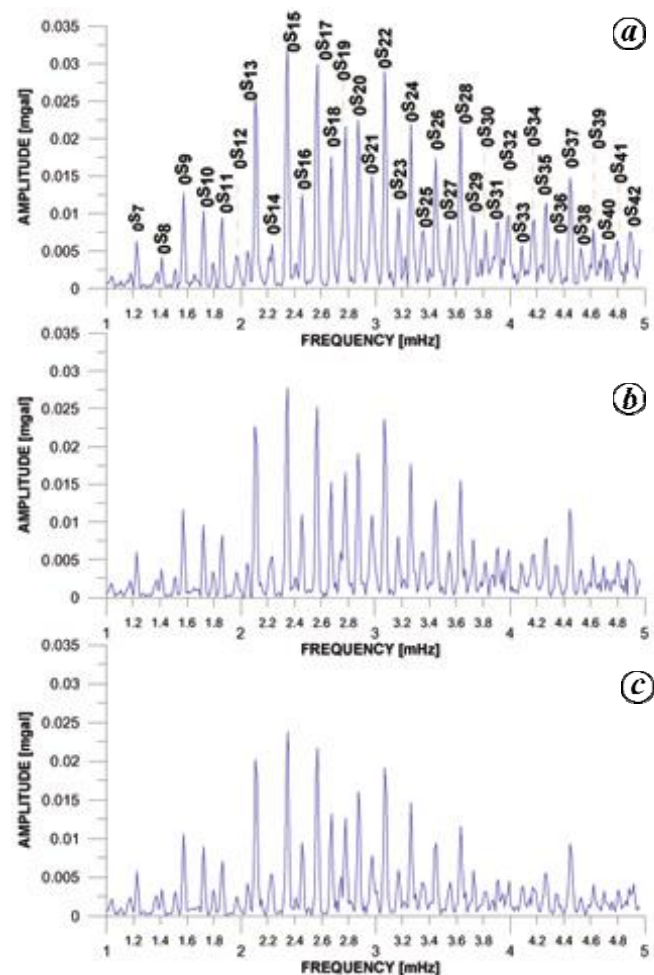


Figure 4. Amplitude spectra of the SG record in India after the Solomon Islands earthquake of magnitude 8.1 using 24 h Hann window (some modes are labelled as shown in *a*). *b*) and *c*) also use 24 h window with a shift of 1.5 h each. In each shift the amplitude of the FOE is decreasing with time.

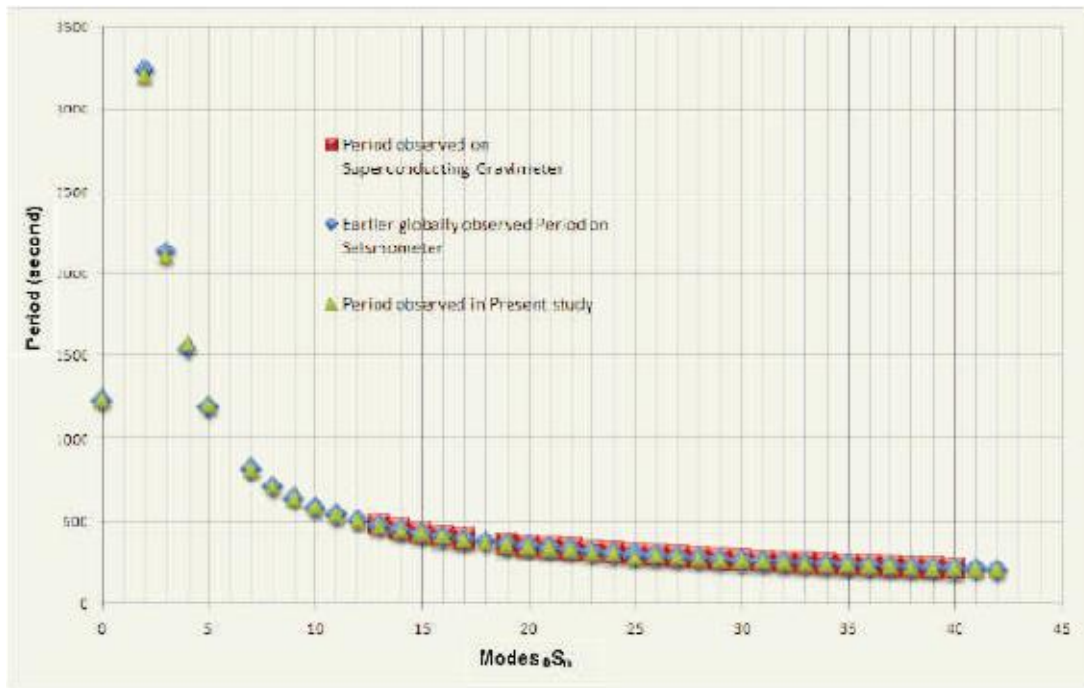


Figure 5. Comparison of periods of the spheroidal modes observed in the present study and earlier global observations.

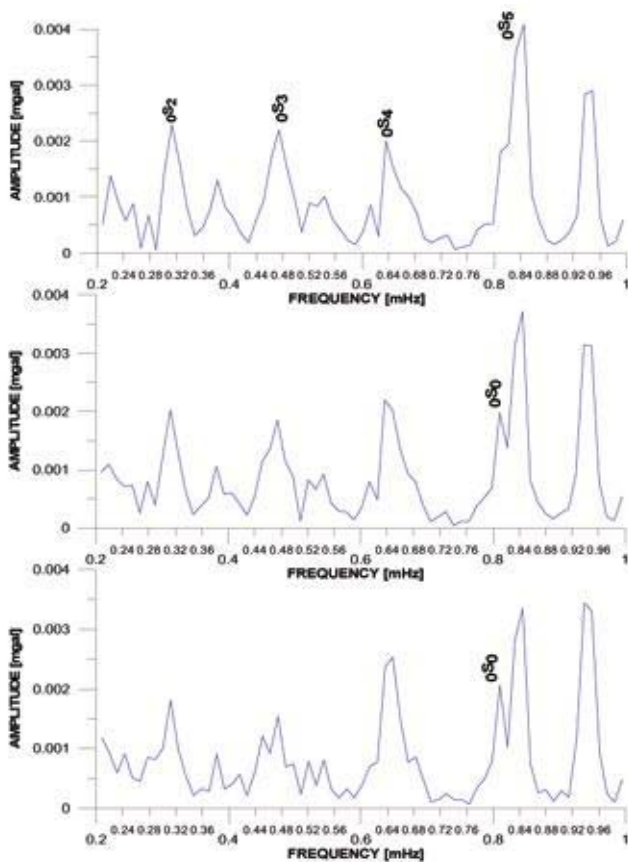


Figure 6. Amplitude spectrum of FOE from 0.2 to 1 mHz band modes for a 24 h window starting at about 4 h after the Solomon Islands earthquake. Periods observed by these modes are not well resolved, but show fair agreement with earlier results.

prominent spheroidal sinusoids decayed by about 10–15% in successive windows. In an earlier study¹¹, this decay pattern from seven successive windows was used to estimate Q , wherein each window of 24 h was shifted by 4 h between successive windows. In the present study because of a gap in the data 31 h after the earthquake, we could only carry out the analysis for three windows, with a total overlap duration of ~ 7 h; this is not sufficient to estimate Q values. However, the excellent agreement of the period of various FOEs and decreasing trend of the amplitudes with increasing time lapsed from the onset of earthquake at the recording site, fully validate the function and resolution of the Indian SG.

Figure 6 shows the amplitude spectrum of seismic oscillation corresponding to the lower modes of the FOE, including the gravest mode ${}_0S_2$, and the breathing mode ${}_0S_0$. The spectra relate to the 24-h time window starting at about 4 h after the earthquake. These lower-order modes, ${}_0S_2$ and ${}_0S_0$, are quite feeble in amplitude and difficult to observe on broadband records of global seismological networks¹². A combination of the low ambient noise level at the site and the high sensitivity of the Indian SG makes it possible to observe these gravest modes. Spectral peaks of these lower-order modes are not as sharp and significant in amplitude as the higher-order modes depicted in Figure 5, but the periods of the modes show reasonable agreement with the earlier studies^{11–13}. Multiple splitting of these peaks may manifest the effect of the earth's rotation on the gravest modes. Subsequent to the Solomon Islands earthquake, the Indian SG has recorded seismic signals of numerous local and regional earthquakes. As a prelude to

Table 1. A comparison of the periods of some fundamental spheroidal modes observed on the Indian superconducting gravimeter after the Solomon Islands earthquake of 1 April 2007 with those determined earlier. The second column shows the values obtained using global data on seismometers^{11,12}, whereas the third column exhibits values observed on a similar instrument¹⁰

Mode ${}_0S_n$	Earlier globally observed period on seismometer	Period observed earlier on Canadian superconducting gravimeter	Period observed in the present study
0	1230		1234
2	3233.11		3200
3	2134.12		2107.30
4	1545.36		1570.19
5	1190.33		1200.00
7	811.11		815.10
8	707.41		708.19
9	633.59		635.31
10	579.17		579.86
11	536.93		536.64
12	402.42		502.32
13	469.56	473.27	474.73
14	445.36	448.26	443.08
15	423.52	426.33	425.62
16	403.73	406.92	407.55
17	387.44	389.56	389.19
18	374.07		374.03
19	358.50	360.20	359.99
20	345.60	347.64	342.86
21	333.59	335.96	336.19
22	323.59	325.23	326.04
23	314.18	315.34	313.04
24	304.22	306.23	306.38
25	295.89	297.72	279.19
26	288.00	289.65	289.93
27	281.43	282.21	282.35
28	274.28	275.20	275.16
29	267.49	268.43	265.85
30	261.02	262.19	260.24
31	254.86	256.05	256.38
32	248.99	250.29	250.43
33	244.06	244.98	244.76
34	238.67	239.70	238.67
35	233.51	234.70	234.15
36	228.57	229.96	229.79
37	224.41	225.24	225.00
38	219.84	220.72	220.41
39	215.46	216.44	215.99
40	211.24	212.49	212.81
41	208.33		208.69
42	204.21		204.25

test whether recorded data include any precursory signals to earthquake occurrence, the current attempts have been aimed at characterizing the time variability of different origins, e.g. dependence on atmospheric pressure and hydrodynamic parameters, etc. Further, some of the large earthquakes from the Sumatra–Java section and elsewhere have excited the FOE. Such datasets, once corrected for tidal and other long-period variations, could permit establishing the true nature of low-order gravest mode.

The usefulness of long-period data in characterizing the weak signals of continually excited FOE has been

already proved by the 3 yr record of SG at Syowa (Antarctica)²⁰. Core mode detection was also attempted²¹ in the long-period temporal variations in gravity in seismic and sub-seismic bands. Recently, even low-amplitude coupled toroidal oscillations were also observed on a single SG data after the Great Sumatra earthquake²². As these findings provide new tools to constraints^{23–25} on our planet's interior composition, mineralogy and dynamics^{4,26–28}, analysis of SG data in long-period seismic bands has opened new perspectives in earth structure studies. Concurrent recordings of the SG and GPS at the recently established MPGO will also help constrain the vertical

displacements, sensitive markers of strain accumulation, with much better resolution than feasible by the GPS data alone^{27,28}. Further, the water-table changes recorded in a well at MPMGO will permit investigations of the hydrological contributions to the gravity data due to seasonal and short spells of intense rainfall, thus making residual gravity data sensitive pointers of stress-induced variations.

By observing the spectral levels in small bands centred on the known frequencies of the normal resonance peaks and comparing them to the spectral levels of ambient noise, it is possible to detect earthquakes at low frequencies, without any knowledge about them at high frequencies. These slow earthquakes were earlier analysed²⁹ on low-frequency seismometers and some 'silent earthquakes' were also detected, which are events with propagation velocities sufficiently low that they do not generate globally detectable waves on high-frequency seismometers. Such events are also likely candidates for study using the Indian SG data in tandem with other instruments around the globe.

1. Arora, B. R., Choubey, V. M., Ajay Paul, Gautam Rawat and Naresh Kumar, Multi-parameter geophysical observatory for earthquake precursory research at Ghuttu, Uttarakhand. In National Workshop on 'Earthquake Precursors', IMD, Ministry of Earth Sciences, New Delhi, 28–29 June 2007.
2. Scholz, C. H., Sykes, L. R. and Agarwal, Y. P., Earthquake prediction: a physical basis. *Science*, 1973, **181**, 803–810.
3. Imanishi, Y., Sato, T., Higashi, T., Sun, W. and Okubo, S., A network of superconducting gravimeters detects submicrogal coseismic gravity changes. *Science*, 2004, **306**, 476–478.
4. Goodkind, J. M., The superconducting gravimeter. *Rev. Sci. Instrum.*, 1999, **70**, 4131–4152.
5. Tiwari, V. M., Singh, B., Vyaghreshwara Rao, M. B. S. and Mishra, D. C., Absolute gravity measurements in India and Antarctica. *Curr. Sci.*, 2006, **91**, 686–689.
6. Prothero, W. A. and Goodkind, J. M., A superconducting gravimeter. *Rev. Sci. Instrum.*, 1968, **39**, 1257–1262.
7. Goodkind, J. M., Continuous measurement of non-tidal variations of gravity. *J. Geophys. Res.*, 1986, **91**, 9425–9434.
8. Richter, B., Das supraleitende Gravimeter, Ph D thesis, Deutsche Geodat. Komm. C 329, Frankfurt am Main, 1987, p. 124.
9. Agnew, D. C., *Earth Tides: An Introduction*, University of California, San Diego, CA, USA, 2005; <http://www.unavco.org:8080/cws/straindata/Notesfrom2005class/tidenote.pdf>
10. Lowrie, W., In *Fundamentals of Geophysics*, Cambridge University Press, Cambridge UK, 1997, pp. 100–101.
11. Kamal and Mansinha, L., A test of the superconducting gravimeter as a long period seismometer. *Phys. Earth Planet. Inter.*, 1992, **71**, 52–60.
12. Sailor, R. V. and Dziewonski, A. M., Measurements and interpretation of normal mode attenuation. *Geophys. J. R. Astron. Soc.*, 1978, **64**, 605–634.
13. Masters, G. and Gilbert, F., Attenuation in the Earth at low frequencies. *Philos. Trans. R. Soc. London*, 1983, **A308**, 479–522.
14. Dziewonski, A. M. and Anderson, D. L., Preliminary reference Earth model. *Phys. Earth Planet. Inter.*, 1981, **25**, 297–356.
15. Valdiya, K. S., *Geology of the Kumaon Lesser Himalaya*, Wadia Institute of Himalayan Geology, Dehradun, 1980, p. 291.
16. Gaur, V. K., Chander, R., Sarkar, I., Khattri, K. N. and Sinval, H., Seismicity and the state of stress from investigations of local earthquakes in the Kumaon Himalaya. *Tectonophysics*, 1984, **118**, 243–251.
17. Khattri, K. N. and Tyagi, A. K., Seismicity patterns in the Himalayan plate boundary and identification of the areas of high seismic potential. *Tectonophysics*, 1983, **96**, 281–297.
18. Bilham, R., Gaur, V. K. and Molnar, P., Himalayan Seismic Hazard. *Science*, 2001, **293**, 1442–1444.
19. Dahlen, F. A., The effect of data windows on the estimation of free oscillation parameters. *Geophys. J. R. Astron. Soc.*, 1982, **69**, 537–549.
20. Nawa, K., Suda, N., Fukao, Y., Sato, T., Aoyama, Y. and Shibuya, K., Incessant excitation of the earth's free oscillations. *Earth Planets Space*, 1998, **50**, 3–8.
21. Hinderer, J. and Crossley, D., Time variations in gravity and inferences on the earth's structure and dynamics. *Surv. Geophys.*, 2000, **21**, 1–45.
22. Xiaogang, H., Lintao, L., Heping, S., Houze, X., Hinderer, J. and Xiaoping, K., Wavelet filter analysis of splitting and coupling of seismic normal modes below 1.5 mHz with superconducting gravimeter records after the 26 December 2004 Sumatra earthquake. *Sci. China, Ser. D, Earth Sci.*, 2006, **49**, 1259–1269.
23. Agnew, D. C. and Farrell, W. E., Self-consistent equilibrium ocean tides. *Geophys. J. R. Astron. Soc.*, 1978, **55**, 171–181.
24. Amalvict, M., Hinderer, J., Boy, J.-P. and Gegout, P., A three year comparison between a superconducting gravimeter (GWRC026) and an absolute gravimeter (FG5#206) in Strasbourg (France). *J. Geodetic Soc. Jpn.*, 2001, **47**, 334–340.
25. Amalvict, M., McQueen, H. and Govind, R., Absolute gravity measurements and calibration of SGCT#31 at Canberra, 1999–2000. *J. Geodetic Soc. Jpn.*, 2001, **47**, 410–416.
26. Amalvict, M., Hinderer, J., Gegout, P., Rosat, S. and Crossley, D., On the use of AG data to calibrate SG instruments in the GGP network. *BIM*, 2002, **135**, 10621–10626.
27. Amalvict, M., Hinderer, J., Makinen, J., Rosat, S. and Rogister, Y., Long-term and seasonal gravity changes and their relation to crustal deformation and hydrology, *J. Geodyn.*, 2004, **38**, 343–353.
28. Amalvict, M., Hinderer, J. and Rozsa, S., Crustal vertical motion along a profile crossing the Rhine graben from the Vosges to the Black Forest Mountains: Results from absolute gravity, GPS and levelling observations. *J. Geodyn.*, 2006, **41**, 358–368.
29. Beroza, G. C. and Jordan, T. H., Searching for slow and silent earthquakes using free oscillations. *J. Geophys. Res.*, 1990, **95**, 2485–2510.

ACKNOWLEDGEMENTS. We thank Prof. V. K. Gaur, Chairman, and members of the Programme Implementation Committee of the Mission Mode Project on Seismology launched by the Department of Science and Technology, Govt of India and currently being steered by the Ministry of Earth Sciences, for their guidance and encouragement. We also thank Dr V. P. Dimri for useful discussions on the application and calibration of the SG. Dr B. K. Bansal is thanked for continued support and advice. Research grants received by A.K. from Indian Institute of Technology, Roorkee are acknowledged. Comments from reviewers on the original manuscript have helped improve the contents.

Received 11 December 2007; revised accepted 8 October 2008